A report on the SCEC project

Using Converted Phases to Image the Bottom of the Los Angeles Basin

Yan Yang and Robert W. Clayton
Seismological Laboratory
Caltech
March 15, 2023

In this report we describe progress on determining the depth of the Los Angeles Basin using the converted seismic phase Sp. This is very much a work in progress and the results should be considered preliminary.

Summary

Converted seismic phases generated by nine deep events beneath or near the Los Angeles Basin (LAB) are used to determine the depth of the LAB by mapping the S-P conversion points. The preliminary results show that the Central Trough of the LAB is 12-14 km deep at its lowest point, which is significantly deeper than the previously assumed value of 9 km (Wright, 1991).

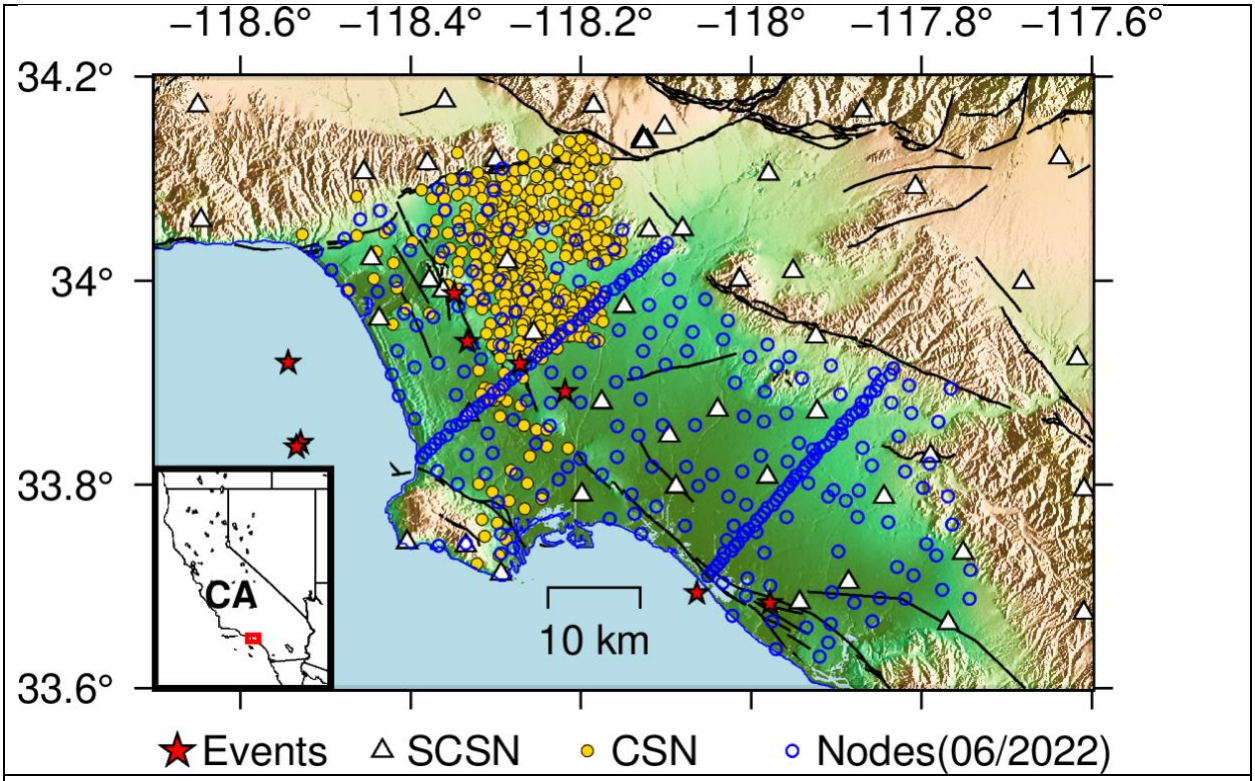

Figure 1. Map of Stations and Earthquakes. A total of 9 earthquakes and 1043 stations

Introduction

One of the least well determined aspects of the LA Basin is its depth. The commonly cited value is 9 km is based on a (sparse) gravity survey reported in 1960, and assumed densities contrasts at the bottom of the basin (McCulloh, 1960). Wright (1991) suggests that a relatively small change in the density contrast could change the depth estimate considerably. A recent study by Muir et al (2022) indicates the northern part of the basin is likely 10 or more km deep, based on an inversion of surface waves from the Ridgecrest event. Apart from general tectonic interest, an accurate estimate of the depth is important for determining the resonant period of the basin for site amplification for the tall buildings in downtown Los Angeles.

In this study, we apply a technique to directly map the sediment-basement interface of the basin by looking for the conversion points where S-waves generated by earthquakes occurring beneath basin are converted to P-waves. The method is similar to the commonly used "receiver functions" but requires some modification because the rays are not near vertical. Fortunately, one of the few locations in S. Californian that has "deep" earthquakes (depth > 12 km) is along the Newport-Inglewood Fault particularly in the Los Angeles basin.

Data and Method

A map showing the locations of the earthquakes and stations used in this study is shown in Figure 1. Nine earthquakes are used, with the details given in Table 1. A total 1043 stations are various types (broardband, nodes and accelerometers) are used. The node array was only deployed during July, 2022, and hence not all earthquakes are recorded by all stations.

Table 1. Events Used in the Study

time	mag	lon0	lat0	depth	evid
2022-06-27T04:13:23.37	2.27	-118.529167	33.841167	10.77	40292048
2022-06-26T16:36:35.59	2.17	-118.534167	33.837167	12.89	40291816
2022-06-26T09:45:05.10	2.28	-118.348667	33.987667	10.96	40291656
2022-06-25T12:42:23.12	1.97	-117.977833	33.683833	11.86	40291224
2022-06-25T10:27:05.84	1.99	-118.543833	33.920000	10.74	40291160
2022-06-22T03:06:10.31	2.03	-118.063667	33.693667	15.90	40288808
2021-04-05T11:44:01.95	4.00	-118.333333	33.940500	19.34	39838928
2021-01-20T16:31:58.95	3.52	-118.271667	33.918667	19.76	39762912
2019-10-18T07:19:51.18	3.54	-118.218500	33.891333	23.63	38905415

An example of the Sp converted phase is shown in Figure 2. It is a clear and isolated phase between the P and S arrivals. It appears primarily on the vertical component at offsets of 5-20 km. All nine events in Table 1 show the Sp phase on (at least) several stations.

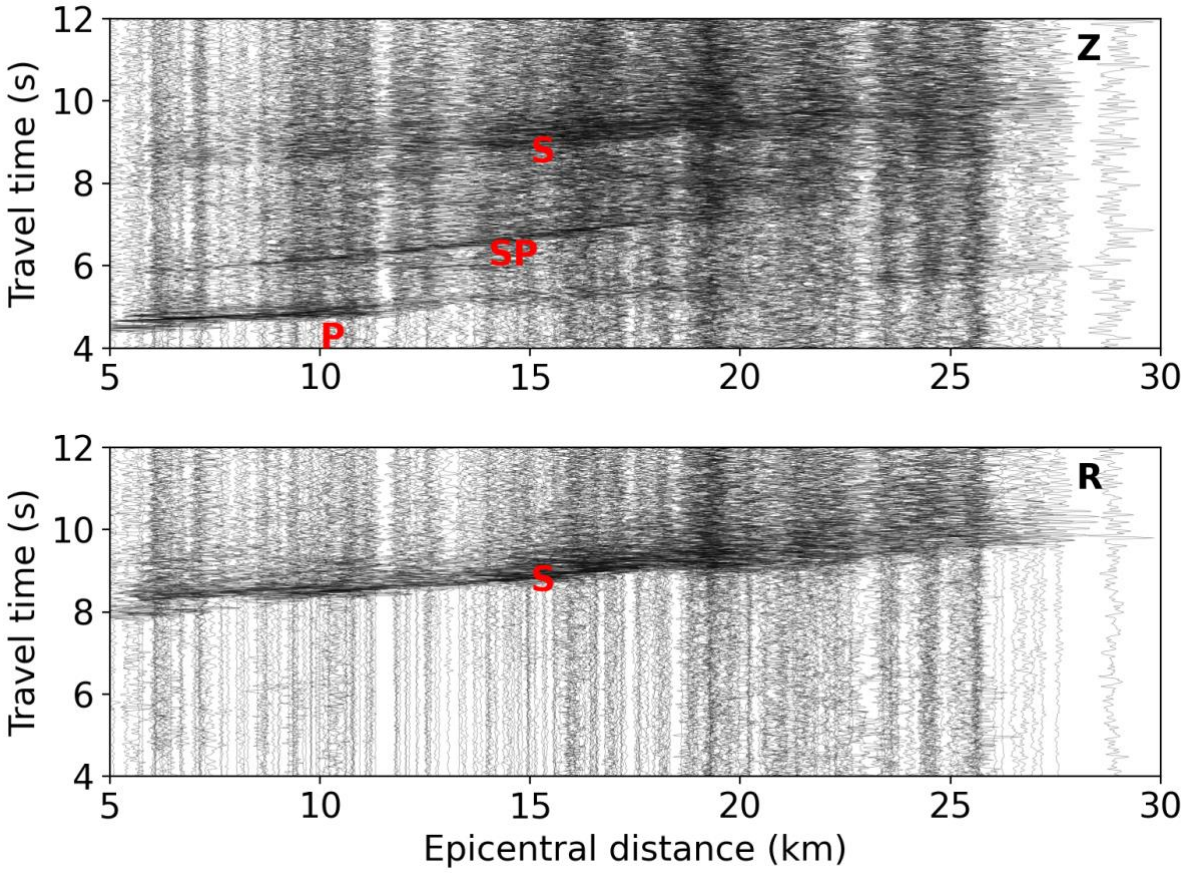

Figure 2. Example of the Sp converted phase. The seismograms are from the 2019/10/18 M3.5 Compton event as recorded on the CSN.

To find the conversion point for a particular source-receiver pair, we use a ray tracing approach with the CVM-S4.26 velocity model. A grid of travel times is calculated on a vertical 2D plane that includes both the earthquake and receiver by first calculating time for an S-wave emanating from the source and then adding to this a P-wave radiating from the receiver. The measured travel time for the Sp phase is then subtracted from this, and consequently the "zero-value" on the grid is the locus possible conversion points. To constrain this curve to a single point we look for the point where the horizontal gradient of the travel time along the ray is equal, which is a way of enforcing Snell's Law, assuming a locally horizontal conversion point. An example of this is shown in Figure 3. Travel time calculations are done with the *pykonal* package.

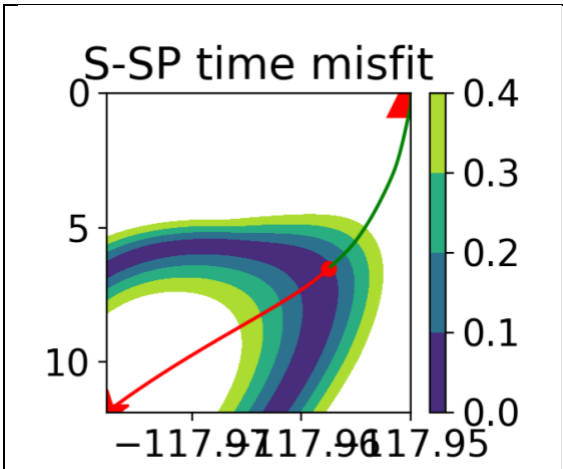

Figure 3. Determining the conversion point. The color contours show the error in the travel times and the red dot is determined as the point that best matches Snell's Law.

We used *PhaseNet* to automatically pick the S-waves, and then manually picked the Sp-phase. A lat-lon grid is then created, and the depths for the conversion points for all source-receiver pairs are stacked on this grid. The coverage and inter-event consistency is shown in Figure 4. The coverage in primarily in the central-northern part of the Central Trough of the LAB, and along the Western Shelf.

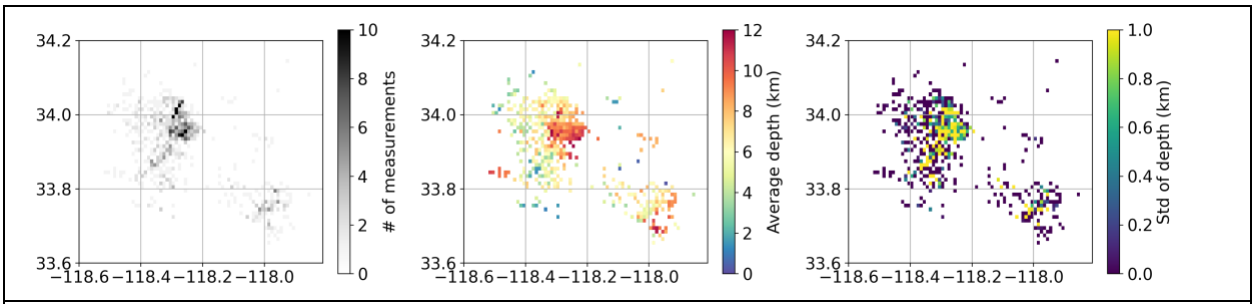

Figure 4. Mapping the conversion points. Left panel shows the coverage of the conversion points. The center panel shows the depths, and the right panel shows the standard deviation of the depth estimates.

The results are displayed in Figure 5, and show that the LAB appears to be 12-14 km at its deepest point in the Central Trough, and about 5-6 km on the Western Shelf. The Newport-Inglewood Fault appears to the a major feature in the topography of the basin bottom, representing a near vertical step of 5-6 km.

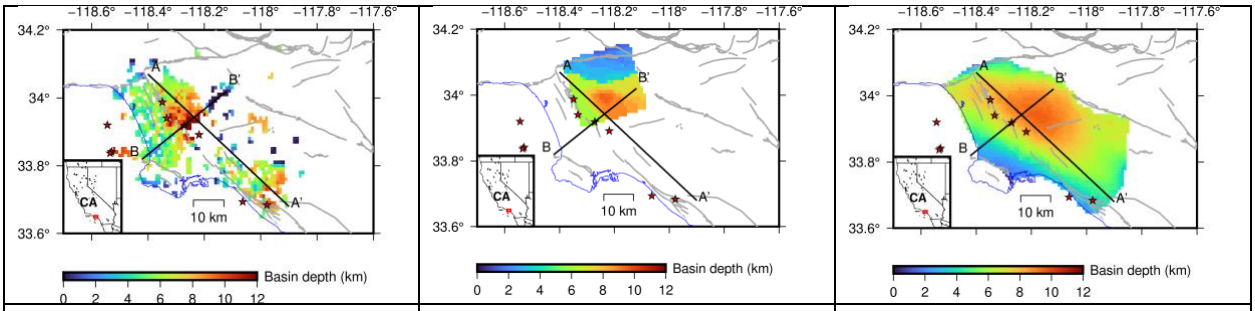

This study	Gravity	Muir et al

Figure 5. Results and Comparison. The left panel shows the results of this study. The centre panel shows the result using gravity with a density contrast chosen to best match the depth of this study. The right panel shows the basin boundary from Muir et al (2022).

Concluding this Project

To complete this project, we plan to try to fill in depth values in the central-southern part of the basin using receiver functions, and to include the results of the LASSIE array (Ma and Clayton, 2016). We also plan to develop and error estimate for the basin depth.

References

Ma, Y, and R. Clayton, (2016), Structure of the Los Angeles Basin from ambient noise and receiver functions, Geophys. J. Int., 206, 1645-1651. doi:10.1093/gji/ggw236

McCulloh, T., (1960), Gravity variations and the geology of the Los Angeles basin of California, USGS Professional Paper 400-B, p. B320-325.

Muir, J., R. Clayton, V. Tsai. and Q. Brissaud, (2022), Parsimonous velocity inversion applied to the Los Angeles Basin, CA, Journal of Geophysics Research: Solid Earth, 127, e2021JB023103, doi:10.1029/2021JB023103

Wright, T. (1991), Structural Geology and tectonic evolution of the Los Angeles basin, California, Act. Margin Basins, 52, 35-134.